ELSEVIER

Biophysical Chemistry 84 (2000) 65–76

Biophysical Chemistry

www.elsevier.nl/locate/bpc

Kinetic study of the oxidation of 3-hydroxyanisole catalysed by tyrosinase

Lorena G. Fenoll[a], José Neptuno Rodríguez-López[a], Ramón Varón[b], Pedro Antonio García-Ruiz[c], Francisco García-Cánovas[a,*], José Tudela[a]

[a] *GENZ: Grupo de Investigación Enzimología, Departamento de Bioquímica y Biología Molecular-A, Facultad de Biología, Universidad de Murcia, E-30100 Murcia, Spain*

[b] *Departamento de Química-Física, Escuela Técnica Superior de Albacete, Universidad de Castilla-La Mancha, Albacete, Spain*

[c] *Departamento de Química Orgánica, Facultad de Química, Universidad de Murcia, Murcia, Spain*

Received 20 July 1999; received in revised form 2 November 1999; accepted 1 December 1999

Abstract

Tyrosinase hydroxylates 3-hydroxyanisole in the 4-position. The reaction product accumulates in the reaction medium with a lag time (τ) which diminishes with increasing concentrations of enzyme and lengthens with increasing concentrations of substrate, thus fulfilling all the predictions of the mechanism proposed by us for 4-hydroxyphenols. The kinetic constants obtained, $k_{cat}^{M} = (46.87 \pm 2.06)\ s^{-1}$ and $K_m^M = (5.40 \pm 0.60)$ mM, are different from those obtained with 4-hydroxyanisole, $k_{cat}^{M} = (184.20 \pm 6.1)\ s^{-1}$ and $K_m^M = (0.08 \pm 0.004)$ mM. The catalytic efficiency, k_{cat}^{M}/K_m^M is, therefore, 265.3 times greater with 4-hydroxyanisole. The possible rate-determining steps for the reaction mechanism of tyrosinase on 3- and 4-hydroxyanisole, based on the NMR spectra of both monophenols, are discussed. These possible rate-determining steps are the nucleophilic attack of hydroxyl's oxygen on the copper and the electrophilic attack of the peroxide on the aromatic ring. Both steps may be of similar magnitude, i.e. take place in the same time scale.

Keywords: Enzyme kinetics; *meta*-Monophenols; *para*-Monophenols; Mushroom tyrosinase

* Corresponding author. Tel.: + 34-968-364782; fax: + 34-968-364147.
E-mail address: canovasf@fcu.um.es (F. García-Cánovas)

0301-4622/00/$ - see front matter
PII: S0301-4622(99)00149-0

1. Introduction

The enzyme tyrosinase (monophenol, *o*-diphenol: oxygen oxidoreductase, EC 1.14.18.1) is of central importance in vertebrate melanine pigmentation. In addition, enzymatic browning in vegetables and fruits is caused by the activity of the tyrosinase present in plant tissues. Tyrosinase plays an important role in fruit and vegetable processing and during the storage of processed foods, catalysing the hydroxylation of monophenols (monophenolase activity) and the oxidation of *o*-diphenols to *o*-quinones (diphenolase activity), both reactions depending on molecular oxygen. The *o*-quinones evolve non-enzymatically to yield several unstable intermediates which polymerise to render melanins [1,2]. The active site of tyrosinase consists of two copper atoms and three states: *met*, *deoxy* and *oxy* [3–10]. Structural models for the active site of these three forms of tyrosinase have been proposed [11–13].

Recently, we studied the reaction of tyrosinase with 4-hydroxyanisole (4HA) using a continuous spectrophotometric method with the cromogenic nucleophile, MBTH [14–19]. This method permitted the kinetic characterisation of 4HA and allowed us to check the fulfilment of the kinetic tests [20,21] for the mechanism previously proposed by us (Scheme 1). The successful application of this method to measure enzymatic activity encouraged us to attempt the first characterisation of a *meta*-hydroxylated substrate such as 3-hydroxyanisole (3HA). The scarcity of information on these class of substrates in the bibliography is possibly due to the instability of the quinonic products originating from the enzyme action on the substrate. Some authors have suggested that tyrosinase shows little enzymatic activity when acting on these substrates [22].

Scheme 1 corresponds to the kinetic reaction mechanism of mushroom tyrosinase on monophenols coupled to non-enzymatic reactions from *o*-quinone. The mechanism is based on previous structural and kinetic mechanisms [12,20,21]. In order to discuss the rate-limiting step in this mechanism, the hydroxylation reaction governed by k_5 was separated into two sub-steps, k_{5_1} and k_{5_2}, which correspond to the nucleophilic attack

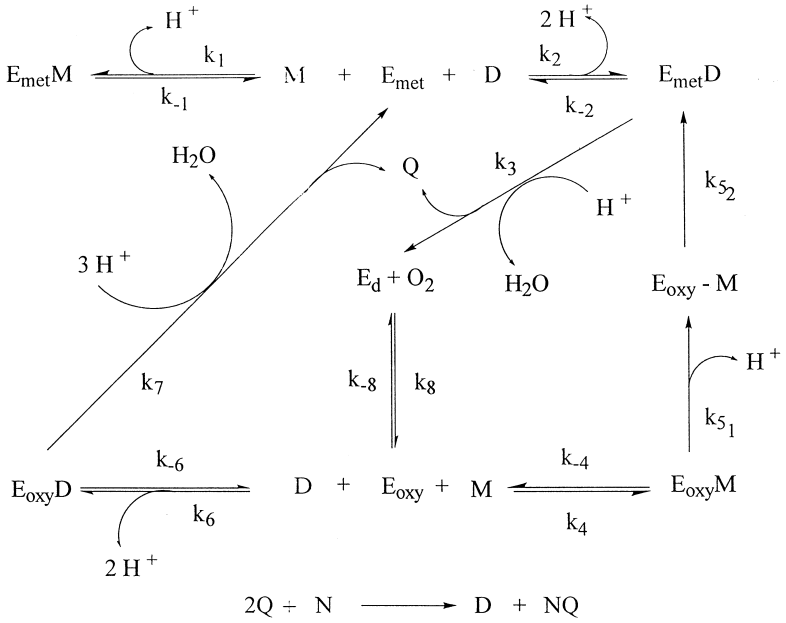

Scheme 1. Kinetic reaction mechanism for the monophenolase activity of tyrosinase coupled to non-enzymatic reactions from *o*-quinone. All the steps are detailed. *Abbreviations*: M, monophenol; D, *o*-diphenol; Q, *o*-quinone; N, nucleophile (MBTH); and NQ, MBTH-quinone adduct.

of the −OH group on the copper and the electrophilic attack of the peroxo unit on the substrate ring, respectively. This division is based on structural and mechanistic studies [12,23]. Several kinetic studies on monophenolase activity concluded that monophenol hydroxylation (governed by k_5) is the rate-limiting step in the mechanism [7,21]. Study of the NMR spectra of 3HA and 4HA may provide useful electron descriptors for predicting the suitability of these compounds as enzyme substrates. Based on these kinetic assays carried out using the above-mentioned method and the NMR studies, 3HA is kinetically characterised and the possible rate-limiting step of the hydroxylation mechanism of monophenols by tyrosinase is discussed.

2. Materials and methods

2.1. Reagents

4HA, 3HA, MBTH and mushroom tyrosinase (8300 U mg^{-1}) were purchased from Sigma (USA). All other chemicals were of analytical grade and supplied by Merck (Germany). Mushroom tyrosinase was purified by the procedure described by Duckworth and Coleman [24]. Protein concentration was determined by the Bradford method [25]. The enzyme concentration was calculated taking a value of M_r 120 000. Stock solutions of the phenolic substrate were prepared in 0.15 mM phosphoric acid to prevent autoxidation. The assay medium contained 50 mM sodium phosphate (pH 6.8), the optimum pH value for mushroom tyrosinase. The acidic character of MBTH required the use of 50 mM buffer in the assay medium [16–19]. A combined system using Milli-RX and Mili-Q Plus (Milipore Corp.) equipment provided type I ultrapure water of 18 MΩ cm, which was used throughout this research.

2.2. Spectrophotometric assays

Absorption spectra were recorded in an ultraviolet-visible Perkin Elmer Lambda-2 spectrophotometer, on-line interfaced with a compatible PC 486DX microcomputer, with a 60-nm/s scanning speed. Temperature was controlled at 25°C using a Haake D1G circulating water-bath with a heater/cooler and checked using a Cole-Parmer digital thermometer with a precision of ±0.1°C. Kinetic assays were also carried out with the above instruments by measuring the appearance of the products in the reaction medium. Reference cuvettes contained all the components except the substrate, with a final volume of 1 ml. All the assays were carried out under saturating conditions of tyrosinase by molecular oxygen, 0.26 mM in the assay medium [26,27].

2.3. Kinetic data analysis

The values of the Michaelis constant (K_m^M) and maximum rate (V_{max}^M) of the enzyme acting on 4HA and 3HA were calculated from triplicate measurements of the steady-state rate (V_{SS}^M) for each initial monophenol concentration ($[4HA]_0$ and $[3HA]_0$). The reciprocals of the variances of V_{SS}^M were used as weighting factors in the non-linear regression fitting of V_{SS}^M vs. $[4HA]_0$ and $[3HA]_0$ data to the Michaelis equation [28]. The fitting was carried out by using a Gauss–Newton algorithm [29] implemented in the Sigma Plot 2.01 program [30].

2.4. NMR assays

^{13}C-NMR spectra of the different monophenols considered here were obtained in a Varian Unity spectrometer of 300 MHz. The spectra were obtained at the optimum pH for mushroom tyrosinase (pH 6.8) and using ^2H_2O as solvent for the substrates. δ values were measured relative to those for tetramethylsilane (δ = 0). The maximum line width accepted in the NMR spectra was 0.06 Hz. Therefore, the maximum accepted error for each peak was ±0.03 ppm.

3. Results and discussion

3.1. Oxidation of 4HA and 3HA by tyrosinase in the presence of MBTH

In previous works [14,15], the oxidation of 4HA

by mushroom tyrosinase at its optimum pH was studied in the presence of MBTH. The action of the enzyme gives rise to the corresponding *o*-quinone, which is attacked by MBTH to produce an adduct with $\lambda_{max} = 492$ nm, which subsequently evolves to show an isobestic point at $\lambda_i = 459$ nm (Fig. 1a). When 3HA was oxidised, a spectrum was obtained with the same maximum and isobestic point (Fig. 1b), confirming that the enzyme hydroxylates in the C-4 position of the benzene ring. The product of both 4HA and 3HA hydroxylation is the same *o*-diphenol, 3,4-dihydroxyanisole. Both monophenols, therefore, produce the same derivates, the *o*-quinone and the adduct, the latter in the presence of MBTH. This is important since the action of the enzyme and the oxidation–reduction reactions which take place [14,15] lead to the accumulation of 3,4-dihydroxyanisole in the medium. Bearing this in mind and also the actuation mechanism of tyrosinase [20,21], all the catalytic steps on the diphenol are common to both monophenols, the only difference being the step in which the respective monophenols participate. After characterising the reaction product, the different kinetic behaviours of the tyrosinase-catalysed oxidation of 3HA were studied in different experimental conditions.

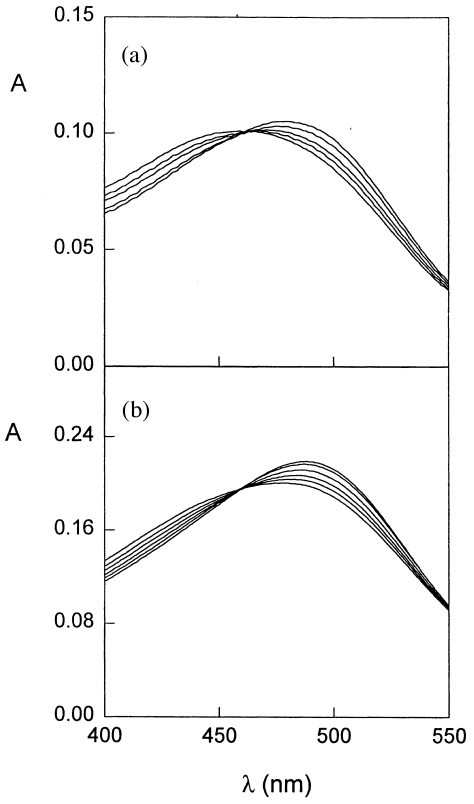

Fig. 1. Spectrophotometric recordings for the oxidation of (a) 4HA and (b) 3HA catalysed by mushroom tyrosinase in the presence the MBTH. Conditions for (a) were 5 μM 4HA, 2% DMF, 2.5 mM MBTH and 24 nM mushroom tyrosinase, and for (b) were 1 mM 3HA, 2% DMF, 2.5 mM MBTH and 2.4 nM mushroom tyrosinase. The assay medium was 50 mM sodium phosphate buffer (pH 6.8) in both cases. At 60 s the reaction was acidified by adding $HClO_4$ for 5 min, followed by addition of NaOH until pH reached 6.8.

3.2. Effect of enzyme concentration

The accumulation of product during the tyrosinase-catalysed oxidation of 3HA showed a lag time (τ), as it did during 4HA oxidation (Fig. 2). An increase in enzyme concentration shortened τ and increased the steady-state rate (V_{SS}^{M}) (Fig. 2), the same behaviour as that observed with all the monophenols studied by this method [16]. This can be explained by the formation of a greater amount of *o*-quinone and the earlier accumulation of the *o*-diphenol needed to reach the steady-state (Scheme 1).

3.3. Effect of monophenol concentration

The value of the τ and the V_{SS}^{M} increased when the substrate concentration was increased (Fig. 3). With increasing monophenol concentration (and a constant enzyme concentration) there was more enzyme in the $E_{met}M$ form (Scheme 1). Thus, the *o*-diphenol concentration required to reach the steady-state increased. Since the system needed more time to reach the steady-state, τ increased. By non-linear regression fitting of V_{SS}^{M} vs. $[3HA]_0$ data, the kinetic constants which characterise the action of tyrosinase on 3HA, at pH 6.8, were determined (see Table 1). This table also shows the values obtained with other 4-hydroxylated substrates.

We shall now turn to the kinetics of the enzymatic oxidation of 3HA in comparison to that of 4HA, by considering the respective NMR spectra.

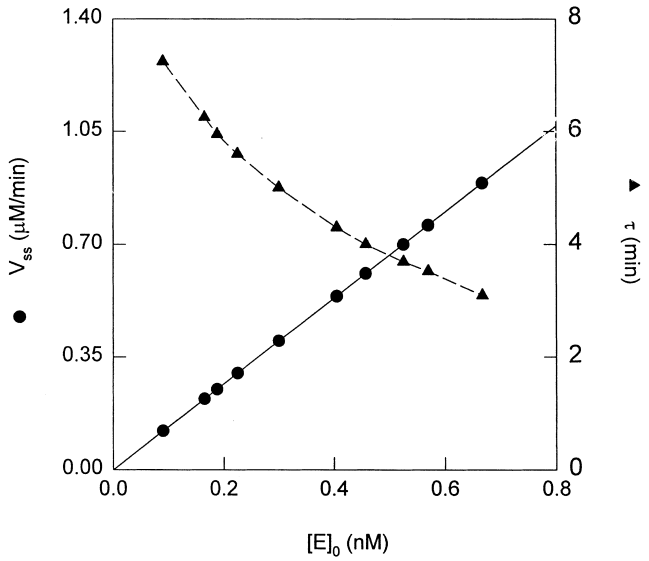

Fig. 2. Dependence of V_{SS} and τ on $[E]_0$ in the oxidation of 3HA catalysed by mushroom tyrosinase in the presence of MBTH. Conditions were: 2% DMF; 2.5 mM MBTH; and 5 mM 3HA in 50 mM sodium phosphate buffer (pH 6.8). (●) Experimental values of V_{SS} vs. $[E]_0$; (—) linear regression fitting of V_{SS} vs. $[E]_0$; and (▲) experimental values of τ vs. $[E]_0$.

The chemical shift (δ) in ^{13}C for a carbon atom is a measurement of its electronic density. This gives information concerning its electrophilic character and, as a consequence, of the degree of nucleophilicity of the oxygen atom belonging to the hydroxyl group at that carbon atom. This has been demonstrated by a number of experimental studies [31–35]. The electron donor capacity of the oxygen atom (nucleophilic power) from different monophenols has been correlated with the experimental δ values of ^{13}C for the carbon atom which supports the OH group [33–35]. The δ values in ^{13}C have been used to corroborate the Hammet values (σ) obtained or to calculate them more accurately [32,33]. Moreover, linear correlations have been demonstrated between δ values in ^{13}C and σ constants, which have been used in both reaction rate and mechanistic studies [31,36]. A low value of δ indicates high electron density of this carbon and so the bound OH will behave like a strong nucleophilic reagent. From Table 2, it can be seen that $\delta_4^p < \delta_3^m$ and so the electron density is greater in C-4 than in C-3. Therefore, these data indicate a more nucleophilic −OH in the *para*-substituted case, 4HA. The same conclusion is obtained by analysing the σ values for both substrates, 0.12 and −0.27 for substituted benzylic alcohol with $-OCH_3$ in the *meta* and *para* position, respectively [37]. Thus, the nucleophilic attack on the copper atoms of tyrosinase in its *met* and *oxy* forms must be more rapid in the case of 4HA than in that of 3HA. In addition,

Table 1
Kinetic constants for the monophenolase activity of mushroom tyrosinase[a]

Monophenol	V_{max}^M (μM min^{-1})	k_{cat}^M (s^{-1})	K_m^M (mM)	k_{cat}^M / K_m^M (mM^{-1} s^{-1})
3HA	1.35 ± 0.06	46.87 ± 2.06	5.40 ± 0.60	8.68 ± 1.34
4HA	5.30 ± 0.03	184.20 ± 6.1	0.08 ± 0.004	2303 ± 191
L-Tyrosine	0.23 ± 0.008	7.98 ± 0.28	0.21 ± 0.01	38.00 ± 3.14

[a] Conditions were as detailed in Fig. 3.

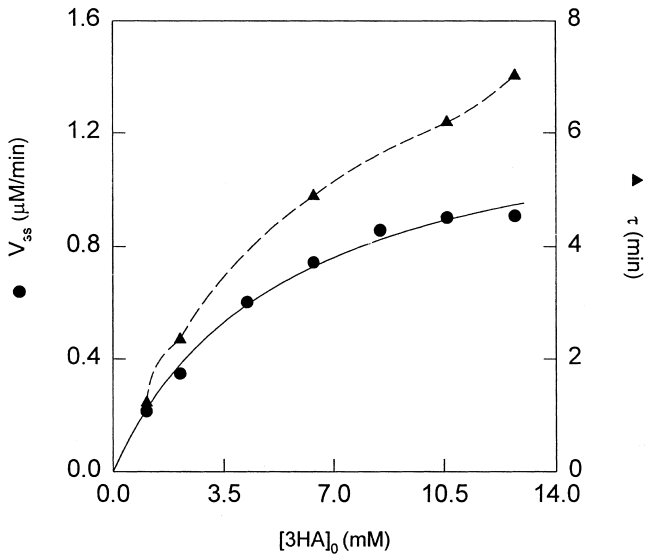

Fig. 3. Dependence of τ and V_{SS} vs. $[3HA]_0$ in the oxidation of 3HA catalysed by mushroom tyrosinase in the presence of MBTH. Conditions were: 2% DMF; 2.5 mM MBTH; and 0.48 nM tyrosinase in 50 mM sodium phosphate buffer (pH 6.8). (●) Experimental values of V_{SS} vs. $[3HA]_0$; (—) non-linear regression fitting of V_{SS} vs. $[3HA]_0$; and (▲) experimental values of τ vs. $[3HA]_0$.

the NMR data were useful for evaluating the electrophilic character of the carbon atom with no hydroxyl group (C-3 in 4HA and C-4 in 3HA). Thus, $\delta_4^m < \delta_3^p$ and so the electron charge density in the C-4 atom of 3HA is greater than in the C-3 atom of 4HA, meaning that the electrophilic attack step will be more rapid in 3HA than in 4HA.

In a previous paper [38] we studied the tyrosinase-catalysed oxidation of 4-hydroxyphenols with different substituents in the carbon-1 (C-1). The difference between the substrates lay in the value of δ_4 since the influence of the substituent in C-1 on the *meta* position was minimal due to similar δ_3 values (Table 2; Espín et al. [38]). We proposed that the limiting step might be the nucleophilic attack of the C-4 hydroxyl on the copper atoms of the active site of the enzyme. If this is correct, the values shown in Table 2 should reveal that $V_{max}^p \gg V_{max}^m$. However, the values are only four times greater in the case of 4HA (Table 1). From these results (Tables 1 and 2), it can be deduced that the nucleophilic and electrophilic attack steps are in the same order of magnitude and, since 3HA favours the electrophilic attack, the differences obtained for V_{max}^M are not surprising. Note (Tables 1 and 2) that substrates that differed in the same ppm in the value of δ_4 show a great difference as regards V_{max}^M since the electrophilic attack step is the same such as L-tyrosine and 4HA.

Table 2
Values of δ_3 and δ_4 for C-3 and C-4, respectively, of the benzene ring of monophenols[a]

Monophenol	δ_3 (ppm)	δ_4 (ppm)
3HA	159.49	110.97
4HA	118.90	152.29
L-Tyrosine	118.08	158.86

[a]Conditions were: saturating substrate concentration in ^2H_2O at pH 7.0; δ values were measured relative to those for tetramethylsilane ($\delta = 0$). The maximum value wide line accepted in the NMR spectra was 0.06 Hz. Therefore, the maximum error accepted for each peak of the spectrum was ±0.03 ppm.

On the other hand, the great difference between $K_m^p = 80$ μM and $K_m^m = 5.4$ mM is difficult to put down to the effect of any step in particular due to the kinetic complexity of the monophenolase mechanism. Nevertheless, the orientation of the substrate in the active site of the enzyme is probably critical in the enzyme–substrate interaction. The *R* substituent in C-1

($-OCH_3$) is the same for both 3HA and 4HA, whose spatial orientation has been studied in the tyrosinase-catalysed oxidation of monophenolic stereoisomers [39,40]. It has been shown that tyrosinase has a greater catalytic affinity (lower K_m^M) towards L-stereoisomers. Thus, the $-OCH_3$ group of 3HA and 4HA must be suitably orientated within the active site. The recently resolved crystal structure of sweet potato catechol oxidase [41], which has no mono-oxygenase activity, indicates that Glu 236 acts as a general base/acid catalyst. However, this residue has no equivalent in human and *Neurospora crassa* tyrosinase, where this amino acid corresponds to glutamine and leucine, respectively. The determination of the three-dimensional structure of a tyrosinase should allow identification of the residue participate as a base/acid catalyst in this type of enzymes with mono-oxygenase activity. The relative orientation of the phenolic −OH with respect to this residue might be worse in 3HA than in 4HA.

Furthermore, since $\delta_3^m > \delta_4^p$, the nucleophilic power is less in 3HA, which might give rise to an increased K_m^M because the dissociation constants of the enzyme and substrate, K_1 and K_4 ($K_1 = k_{-1}/k_1$ and $K_4 = k_{-4}/k_4$), would increase as the values of the second-order rate constants k_1 and k_4 decreased. These results can also be explained by the analytical expressions for V_{max}^M and K_m^M, for which reason we made the following kinetic analysis.

3.4. Kinetic analysis

As stated above, the *o*-diphenol which is formed, regenerated and accumulated in the reaction medium (Scheme 1), is the same in the case of both monophenols, 3,4-dihydroxyanisole. This encouraged us to carry out a kinetic analysis for both monophenols since the rate constants of the diphenolase route are the same, and this would permit us to compare the hydroxylase cycles of both monophenols [20].

The equation for the velocity of the reaction mechanism (Scheme 1) is:

$$V_{SS}^M = \frac{b_0[D]_{SS}[O_2]_0[E]_0}{c_0 + c_1[O_2]_0 + c_2[M]_0[O_2]_0 + c_3[D]_{SS}[O_2]_0} \quad (1)$$

where $[M]_0$ and $[O_2]_0$ are the initial monophenol and oxygen concentrations, and $[D]_{SS}$ represents the diphenol accumulated in the steady-state, with:

$$b_0 = 2k_{5_2}k_3k_7K_4$$

$$c_0 = k_{5_2}k_3K_8K_4K_6$$

$$c_1 = k_{5_2}(3k_7K_2 + k_3K_6)K_4$$

$$c_2 = 3k_{5_2}k_7K_2K_4(1/K_1) + k_3(k_{5_2} + k_{5_1})K_6$$

$$c_3 = k_{5_2}(k_3 + 3k_7)K_4$$

$$R = \frac{[D]_{SS}}{[M]_0}$$

with,

$$R = k_{5_1}K_6/2k_7K_4$$

and the equilibrium constants:

$$K_1 = k_{-1}k_1,\ K_2 = k_{-2}/k_2,\ K_4 = k_{-4}/k_4,\ K_6 = k_{-6}/k_6$$

As the oxygen concentration is saturating, Eq. (1) can be simplified to:

$$V_{SS}^M = \frac{b_0[D]_{SS}[E]_0}{c_1 + c_2[M]_0 + c_3[D]_{SS}} = \frac{b_0R[M]_0[E]_0}{c_1 + [c_2 + c_3R][M]_0} \quad (2)$$

Thus,

$$V_{max}^M = b_0R[E]_0/(c_2 + c_3R) \quad (3)$$

$$K_m^M = c_1/(c_2 + c_3R) \quad (4)$$

Table 3
Equations describing the dependencies of the kinetic constants on rate and binding constants of the reaction mechanism of tyrosinase

Kinetic constant (Eqn. no.)	i	α_I	β_i
(9) $V_{max}^{M} = \frac{\alpha_1 k_{51}}{\beta_1 + k_{51}}$	1	$\frac{2k_3k_7k_{52}[E]_0}{2k_3k_7 + k_{52}(k_3 + 3k_7)}$	$\frac{6k_{52}{k_7}^2K_2K_4 + 2k_3k_7k_{52}K_1K_6}{2k_3k_7K_1K_6 + k_{52}(k_3 + 3k_7)K_1K_6}$
(10) $V_{max}^{M} = \frac{\alpha_2 k_{52}}{\beta_2 + k_{52}}$	2	$\frac{2k_3k_7k_{51}K_1K_6[E]_0}{6{k_7}^2K_2K_4 + 2k_3k_7K_1K_6 + k_{51}(k_3 + 3k_7)K_1K_6}$	$\frac{2k_3k_7k_{51}K_1K_6}{6{k_7}^2K_2K_4 + 2k_3k_7K_1K_6 + k_{51}(k_3 + 3k_7)K_1K_6}$
(11) $K_m^{M} = \frac{\alpha_3 k_{52}}{\beta_3 + k_{52}}$	3	$\frac{2k_7(3k_7K_2 + k_3K_6)K_1K_4}{6{k_7}^2K_2K_4 + 2k_3k_7K_1K_6 + k_{51}(k_3 + 3k_7)K_1K_6}$	$\frac{2k_3k_7k_{51}K_1K_6}{6{k_7}^2K_2K_4 + 2k_3k_7K_1K_6 + k_{51}(k_3 + 3k_7)K_1K_6}$
(12) $K_m^{M} = \frac{\alpha_4 K_4}{\beta_4 + K_4}$	4	$\frac{(3k_7K_2 + k_3K_6)K_1}{3k_7K_2}$	$\frac{2k_3k_7(k_{51} + k_{52})K_1K_6 + k_{51}k_{52}(k_3 + 3k_7)K_1K_6}{6k_{52}{k_7}^2K_2}$

Substituting the values of b_0, c_1, c_2, c_3 and R in Eqs. (3) and (4) gives:

$$V^M_{max} = \frac{2k_3k_{5_1}k_{5_2}k_7K_1K_6[E]_0}{6k_{5_2}k_7^2K_2K_4 + 2k_3k_7(k_{5_1}+k_{5_2})K_1K_6 + k_{5_1}k_{5_2}(k_3+3k_7)K_1K_6} \quad (5)$$

$$K^M_m = \frac{2k_{5_2}k_7(3k_7K_2+k_3K_6)K_1K_4}{6k_{5_2}k_7^2K_2K_4 + 2k_3k_7(k_{5_1}+k_{5_2})K_1K_6 + k_{5_1}k_{5_2}(k_3+3k_7)K_1K_6} \quad (6)$$

The catalytic efficiency being:

$$k^M_{cat}/K^M_m = k_3k_{5_1}K_6/[(3k_7K_2+k_3K_6)K_4] \quad (7)$$

and the relation between the catalytic efficiencies of a *p*-hydroxyphenol and its corresponding *m*-hydroxyphenol is:

$$\frac{(k^M_{cat}/K^M_m)^p}{(k^M_{cat}/K^M_m)^m} = \frac{k^p_{5_1}K^m_4}{k^m_{5_1}K^p_4} = \frac{k^p_{5_1}k^m_{-4}k^p_4}{k^m_{5_1}k^p_{-4}k^m_4} \quad (8)$$

From the analytical expressions deduced for V^M_{max} and K^M_m [Eqs. (5) and (6)], their dependence on the transformation constants and the binding constants of the monophenolase pathway can be established (Table 3). Thus, the V^M_{max} value depends hyperbolically on both k_{5_1} and k_{5_2}. However, the K^M_m value only depends hyperbolically on k_{5_2} but also depends on K_4.

3.5. Catalytic speed

In light of the these simplified equations it is possible to understand the data obtained for 4HA and 3HA (Table 1) with respect to the NMR data (Table 2). Thus, 4HA has a low δ^p_4 value (Table 2), meaning that the strength of the nucleophilic attack of the oxygen in the hydroxyl at C-4 must be substantial and so the value of $k^p_{5_1}$ and V^M_{max} must also be high [Eq. (9)]. The value of δ^p_3 is high (Table 2), so the electron density in C-3 must be low, and therefore, the constant of the electrophilic attack of the oxygen of the *oxy* form on C-3 ($k^p_{5_2}$) will be low. This will carry out a low V^M_{max} [Eq. (10)]. These considerations suggest a direct but opposite influence of both reactions steps in the V^M_{max} value of the enzyme in its action on 4HA.

In the case of 3HA, the value of δ^m_3 is high and so the electron density at C-3 is low. The nucleophilic activity of the hydroxyl oxygen towards the coppers of the active site is low and $k^m_{5_1}$ falls, which would bring about a low V^M_{max} [Eq. (9)]. The value of δ^m_4 is low (Table 2), which means the electron density in C-4 is high. Thus, the electrophilic attack of the oxygen of the *oxy* form (Scheme 1) must be rapid, increasing $k^m_{5_2}$ and V^M_{max} [10]. This means that the fall in V^M_{max} associated with the fall in $k^m_{5_1}$, is matched by the rise in $k^m_{5_2}$ and so the overall fall in V^M_{max} is only fourfold (Table 1). From these data it may be gathered that the value of k_{5_2} is not much greater than that of k_{5_1} since the acceleration of k_{5_2} in 3HA does not influence V^M_{max} much. In other words, the two steps must have rate constant values of the same order of magnitude.

3.6. Catalytic affinity

The values of K^M_m shown in Table 1 can be explained by Eqs. (11) and (12) and taking in to account the data of Table 2. Thus, since $\delta^p_3 > \delta^m_4$ (Table 2), the charge density is greater in C-4 of 3HA than in C-3 of 4HA, the electrophilic attack is favoured in 3HA and K^M_m increases [Eq. (11) and Table 1]. Since K^M_m depends hyperbolically on the dissociation constant of the *oxy* form of the enzyme with the monophenol (Scheme 1) K^M_m would increase as K_4 increases [Eq. (12)].

The substrate must bind with the enzyme before making a nucleophilic attack on the copper atoms of the active site of tyrosinase (Scheme 1). We suggest that in this enzyme–substrate complex the hydrogen of the phenolic OH might bind with an amino acid of the active site such as a histidine. It is known that at low pH where the histidine is protonated K^M_m increases, while activity diminishes [16]. Therefore, the putative hydrogen bond between the nitrogen of the histidine and the hydrogen of the phenolic OH might facilitate the nucleophilic attack of the oxygen on the

copper. The hydrogen bond with the histidine would be favoured by the nucleophilic power of the phenolic oxygen in the 4HA. This would imply a high k_4^p value and low K_4^p value, so that K_m^M would be low [Eq. (11)]. The opposite would occur in 3HA with a low k_4^m implying a high K_4^m, with K_m^M increasing [Eq. (12)]. Thus, in the case of 3HA, k_{5_2} and K_4 would increase, resulting in a stronger increase in K_m^M than in 4HA (Table 1).

3.7. Catalytic efficiency

From Eq. (7) it can be established that the catalytic efficiency is directly proportional to the rate constant of the nucleophilic attack (k_{5_1}) and inversely proportional to the dissociation constant of the *oxy* form with the monophenol (K_4). The data shown in Table 1 for the catalytic efficiencies are in accordance with Eq. (7). Thus, $k_{5_1}^p > k_{5_1}^m$ and $K_4^p < K_4^m$ and therefore, $(k_{\text{cat}}^p/K_m^p) \gg (k_{\text{cat}}^m/K_m^m)$. Note that the catalytic efficiency does not depend on the rate of the electrophilic attack and that it is much lower for 3HA (Table 1). Moreover, the ratio between the catalytic efficiencies of both *para* and *meta* monophenols depend on the rate of the nucleophilic attack ($k_{5_1}^m$,$k_{5_1}^p$) and the association/dissociation constants (K_4^m,K_4^p) [Eq. (8)]. From the results observed in Table 1, the ratio between both catalytic efficiencies was calculated to be 265.3; such a value agrees with the above discussion.

To summarise, we have kinetically characterised a tyrosinase substrate hydroxylated in *meta* position, 3HA. A comparison with its hydroxylated isomer in the *para* position, 4HA, points to small differences in $V_{\max}^M$ and large differences in K_m^M. The efficiency of the enzyme on 3HA is much less than on 4HA. These results suggest the existence of physiological routes, such as melanin biosynthesis, with good catalytic efficiency arising from *p*-hydroxylated rather than *m*-hydroxylated phenolic compounds of tyrosinase.

4. Nomenclature

C-1: Carbon atom in the 1-position of the benzene ring
C-3: Carbon atom in the 3-position of the benzene ring
C-4: Carbon atom in the 4-position of the benzene ring
δ_3: Chemical displacement value at C-3
δ_4: Chemical displacement value at C-4
D: *o*-Diphenol
$[D]_{SS}$: *o*-Diphenol concentration in the steady-state
DMF: *N*,*N*′-dimethylformamide
ε_I: Molar absorptivity at λ_i
$[E]_0$: Initial tyrosinase concentration
E_d: *desoxy*tyrosinase
E_{met}: *met*tyrosinase (with Cu^{2+}–Cu^{2+} in the active site)
E_{oxy}: *oxy*tyrosinase with Cu^{2+}–O_2^{2-}–Cu^{2+} in the active site
3HA: 3-Hydroxyanisole
4HA: 4-Hydroxyanisole
λ_i: Wavelength at the isosbestic point
$\lambda_{\max}$: Wavelength at the maximum of absorbance
K_m^M: Apparent Michaelis constant of tyrosinase towards monophenols
k_{cat}^M: Catalytic constant of tyrosinase towards monophenols
K_1: k_{-1}/k_1
K_2: k_{-2}/k_2
$[M]_0$: Initial monophenol concentration
MBTH: 3-Methyl-2-benzothiazolinone hydrazone
NMR: Nuclear magnetic resonance
PB: Sodium phosphate buffer
$[O_2]_0$: Initial oxygen concentration
V_{SS}^M: Steady-state rate of tyrosinase towards monophenols
$V_{\max}^M$: Maximum steady-state rate of tyrosinase towards monophenols

Acknowledgements

This work was supported in part by the CICYT (Spain), Project ALI96-1111-C04. JNR-L is also supported by this project, and LGF has a fellowship from Fundación Séneca, Comunidad Autónoma de Murcia.

References

[1] D.A. Robb, in: R. Lontie (Ed.), Copper Proteins and Copper Enzymes, CRC Press, 1984, p. 207.

[2] G. Prota, M. d'Ischia, A. Napolitano, in: J.J. Nordlund, R. Boissy, V. Hearing, R. King, J.P. Ortonne (Eds.), The Pigmentary System, Univ. Press, Oxford, 1998, p. 307.

[3] H.S. Mason, Structure and functions of the phenolase complex, Nature 177 (1956) 79–81.

[4] R.L. Jolley Jr., L.H. Evans, H.S. Mason, Reversible oxygenation of tyrosinase, Biochem. Biophys. Res. Commun. 46 (1972) 878–884.

[5] A.J. Schoot-Uiterkamp, H.S. Mason, Magnetic dipole–dipole coupled Cu(II) pairs in nitric oxide-treated tyrosinase: a structural relationship between the active sites of tyrosinase and hemocyanin, Proc. Natl. Acad. Sci. U.S.A. 70 (1973) 993–996.

[6] R.L. Jolley Jr., L.H. Evans, N. Makino, H.S. Mason, Oxytyrosinase, J. Biol. Chem. 249 (1974) 335–345.

[7] N. Makino, H.S. Mason, Reactivity of oxytyrosinase towards substrates, J. Biol. Chem. 248 (1973) 5731–5735.

[8] N. Makino, P. McMahill, H.S. Mason, T.H. Moss, The oxidation state of copper in resting tyrosinase, J. Biol. Chem. 249 (1974) 6062–6066.

[9] A.J. Schoot-Uiterkamp, L.H. Evans, R.L. Jolley, H.S. Mason, Absorption and circular dichroism spectra of different forms of mushroom tyrosinase, Biochim. Biophys. Acta 453 (1976) 200–204.

[10] K. Lerch, in: H. Sigel (Ed.), Metal Ions in Biological Systems, Marcel Dekler, New York, 1981, p. 143.

[11] E.I. Solomon, M.D. Lowery, Electronic structure contributions to function in bioinorganic chemistry, Science 259 (1993) 1575–1581.

[12] E.I. Solomon, U.M. Sundaram, T.E. Machonkin, Multicopper oxidases and oxygenases, Chem. Rev. 96 (1996) 2563–2605.

[13] C.W.G. Van Gelder, W.H. Flurkey, H.J. Wichers, Sequence and structural features of plant and fungal tyrosinases, Phytochemistry 45 (1997) 1309–1323.

[14] J.C. Espín, R. Varón, J. Tudela, F. García-Cánovas, Kinetic study of the oxidation of 4-hydroxyanisole catalysed by tyrosinase, Biochem. Mol. Biol. Int. 41 (1997) 1265–1276.

[15] J.C. Espín, J. Tudela, F. García-Cánovas, 4-Hydroxyanisole: the most suitable monophenolic substrate for determining spectrophotometrically the monophenolase activity of polyphenol oxidase from fruits and vegetables, Anal. Biochem. 259 (1998) 118–126.

[16] J.N. Rodríguez-López, J. Escribano, F. García-Cánovas, A continuous spectrophotometric method for the determination of monophenolase activity of tyrosinase using 3-methyl-2-benzothializone hydrazone, Anal. Biochem. 216 (1994) 205–212.

[17] J.C. Espín, M. Morales, R. Varón, J. Tudela, F. García-Cánovas, A continuous spectrophotometric method for determining the monophenolase and diphenolase activities of apple polyphenol oxidase, Anal. Biochem. 231 (1995) 237–246.

[18] J.C. Espín, M. Morales, R. Varón, J. Tudela, F. García-Cánovas, A continuous spectrophotometric method for determining the monophenolase and diphenolase activities of pear polyphenol oxidase, J. Food Sci. 61 (1996) 1177–1182.

[19] J.C. Espín, M. Morales, P.A. García-Ruiz, J. Tudela, F. García-Cánovas, Improvement of a continuous spectrophotometric method for determining the monophenolase and diphenolase activities of mushroom polyphenol oxidase, J. Agric. Food Chem. 45 (1997) 1084–1090.

[20] J.N. Rodríguez-López, J. Tudela, R. Varón, F. García-Cánovas, F. García-Carmona, Analysis of a kinetic model for melanin biosynthesis pathway, J. Biol. Chem. 267 (1992) 3801–3810.

[21] J.R. Ros, J.N. Rodríguez-López, F. García-Cánovas, Tyrosinase: kinetic analysis of the transient phase and the steady state, Biochim. Biophys. Acta 1204 (1994) 33–42.

[22] S. Passi, M. Nazzaro-Porro, Molecular basis of substrate and inhibitory specificity of tyrosinase: phenolic compounds, Br. J. Dermatol. 104 (1981) 659–665.

[23] D.E. Wilcox, A.G. Porras, Y.T. Hwang, K. Lerch, M.E. Winkler, E.I. Solomon, Substrate analogue binding to the coupled binuclear copper active site in tyrosinase, J. Am. Chem. Soc. 107 (1985) 4015–4027.

[24] H.W. Duckworth, J.E. Coleman, Physicochemical and kinetic properties of mushroom tyrosinase, J. Biol. Chem. 245 (1970) 1613–1625.

[25] M.M. Bradford, A rapid and sensitive method for the quantification of microgram quantities of proteins utilizing the principle of protein-dye binding, Anal. Biochem. 72 (1976) 248–256.

[26] J.N. Rodríguez-López, J.R. Ros, R. Varón, F. García-Cánovas, Calibration of a Clark-type oxygen electrode by tyrosinase-catalyzed oxidation of 4-*tert*-butylcathechol, Anal. Biochem. 202 (1992) 356–360.

[27] J.N. Rodríguez-López, J.R. Ros, R. Varón, F. García-Cánovas, Oxygen Michaelis constants for tyrosinase, Biochem. J. 293 (1993) 859–866.

[28] M.L. Johnson, Non-linear least-squares analysis, Methods Enzymol. 240 (1994) 1–22.

[29] D.W. Marquardt, An algorithm for least-squares estimation of nonlinear parameters, J. Soc. Ind. Appl. Math. 11 (1963) 431–441.

[30] Jandel Scientific, Sigma Plot 2.01 for Windows, Jandel Scientific, Corte Madera, 1994.

[31] G.C. Levy, G.L. Nelson, Resonancia Magnética Nuclear de carbono 13 para quimicos orgánicos, Bellaterra SA, Barcelona, 1976, p. 100.

[32] S. Marriot, R.D. Topsom, A theoretical scale of substituent resonance parameters (σ_R^o), J. Chem. Soc. Perkin Trans. II (1985) 1045–1047.

[33] J. Bromilow, R.T.C. Brownlee, V.O. Lopez, R.W. Taft, *Para*-substituent carbon-13 chemical shifts in substituted benzenes, J. Org. Chem. 44 (1979) 4766–4770.

[34] J. Antosiewicz, J. McCammon, M.K. Gilson, The determinants of pK_as in proteins, Biochemistry 35 (1996) 7819–7833.
[35] S. Tomiyama, S. Sakai, T. Nihiyama, F. Yasmada, Factors influencing the antioxidant activities of phenols by an ab initio study, Bull. Chem. Soc. Jpn. 66 (1993) 205–211.
[36] T. Shogo, S. Shogo, N. Tomihiro, Y. Fukiko, Factors influencing the antioxidant activities of phenols by an ab initio study, Bull. Chem. Soc. Jpn. 66 (1993) 299–304.
[37] C. Hansch, A. Leo, Substituents Constants for Correlation Analysis in Chemistry and Biology, John Wiley & Sons, New York, 1979, p. 86.
[38] J.C. Espín, P.A. García-Ruiz, J. Tudela, R. Varón, F. García-Cánovas, Monophenolase and diphenolase reaction mechanisms of apple and pear polyphenol oxidases, J. Agric. Food Chem. 46 (1998) 2968–2975.
[39] J.C. Espín, P.A. García-Ruiz, J. Tudela, F. García-Cánovas, Study of stereospecificity in mushroom tyrosinase, Biochem. J. 331 (1998) 547–551.
[40] J.C. Espín, P.A. García-Ruiz, J. Tudela, F. García-Cánovas, Study of stereospecifity in pear and strawberry polyphenol oxidases, J. Agric. Food Chem. 46 (1998) 2469–2473.
[41] T. Klabunde, C. Eicken, J.C. Sacchettini, B. Krebs, Crystal structure of a plant catechol oxidase containing a dicopper center, Nature Struct. Biol. 5 (1998) 1084–1090.